PHYSICAL REVIEW B **82**, 075404 (2010)

Role of electronic friction during the scattering of vibrationally excited nitric oxide molecules from Au(111)

Serge Monturet and Peter Saalfrank
Institut für Chemie, Universität Potsdam, Karl-Liebknecht-Strasse 24-25, D-14476 Potsdam-Golm, Germany
(Received 31 May 2010; revised manuscript received 13 July 2010; published 5 August 2010)

Some time ago, it has been observed that vibrationally highly excited NO(v) molecules (with typical vibrational quantum numbers $v \approx 15$) lose substantial amounts of vibrational energy when scattering off a Au(111) surface [H. Huang, C. Rettner, D. Auerbach, and A. Wodtke, Science **290**, 111 (2000)]. This has been interpreted as a sign for the breakdown of the Born-Oppenheimer approximation due to vibration-electron coupling. It has been argued that this process cannot be understood on the basis of single-quantum transitions which are typical for "electronic friction" models based on a perturbative treatment of weak vibration-electron couplings. Rather, multiple-quanta transitions characteristic for strong nonadiabatic effects are needed according to recent classical surface hopping calculations involving multiple potential-energy surfaces and model Hamiltonians [N. Shenvi, S. Roy, and J. C. Tully, Science **326**, 829 (2009)]. Here we address the importance and magnitude of electronic friction for NO@Au(111) by using fully quantum-mechanical, parameter-free first-principles theories in reduced dimensions. Periodic density-functional theory calculations are performed to obtain a ground-state potential-energy surface along the desorption and NO-vibration coordinates, and coordinate-resolved, finite NO vibrational lifetimes due to vibration-electron coupling. Using this input, the scattering event is modeled by open-system density-matrix theory in the frame of the coupled-channel-density-matrix method, which allows for the inclusion of energy relaxation of the scattering NO molecules. It is found that within this model at least, electronic friction accounts for the observed vibrational deactivation of NO scattering from gold.

DOI: 10.1103/PhysRevB.82.075404 PACS number(s): 68.49.Df, 68.43.Pq, 82.20.Kh, 31.70.Hq

I. INTRODUCTION

In almost all calculations dealing with the dynamics of molecules at surfaces, the Born-Oppenheimer approximation (BOA) (Ref. 1) is first assumed, by which the full Schrödinger equation is separated in electronic and nuclear parts. This considerably simplifies dynamical simulations, e.g., of (reactive) scattering of small molecules from metal surfaces,[2–5] in which case motion on only a single (the ground state) potential-energy surface is considered.

However, in particular, at metal surfaces with their characteristic electronic excitation continuum and/or in the case of highly excited scatterers, the BOA becomes questionable. Rather, the inclusion of electronically excited states, either directly (by multiple-state models) or indirectly (by electronic friction models) can become important. For example, in experiments of Huang *et al.*[6] on highly vibrationally excited NO(v) molecules scattering from Au(111) surfaces, strong nonadiabatic behavior has been suggested to be the main cause for the observed, pronounced vibrational deactivation: When starting with initial vibrational quantum numbers $v \approx 15$ and an initial kinetic energy of $E_k = 0.05$ eV), the authors found a broad, relaxed vibrational energy distribution for scattered NO with an average loss of 7–8 vibrational quanta, corresponding to ≈ 1.5 eV. In contrast, NO scattering from insulating LiF showed very little vibrational relaxation. Further, electron-emission from Au(111) covered with the low-work function metal Cs was observed during scattering.[7] All of this demonstrates that nonadiabatic couplings play an important role: In metals, electronic excitations can be created, by simultaneously transferring the energy of vibrating molecules to the surface.

While highly excited NO scattering from gold loses multiple vibrational quanta, single-quantum relaxation dominates for small adsorbed molecules when excited to low vibrational levels. A classic example is CO on Cu(100), whose internal stretch mode decays from CO($v=1$) to CO($v=0$) within about 2 ps.[8] This process is also believed to be dominated by non-Born-Oppenheimer coupling between vibrational and electronic degrees of freedom, and is typically modeled via Fermi's golden rule. Accordingly, the transition rate between vibrational levels $|v\rangle$ and $|u\rangle$ is, at $T=0$, given by[9]

$$\Gamma_{v\to u} = \frac{2\pi}{\hbar} \sum_i \sum_f |\langle v,i|\hat{T}_{nuc}|u,f\rangle|^2 \delta(\varepsilon_i - \varepsilon_f + \hbar\omega_{vu}). \quad (1)$$

Here, $|i\rangle$ and $|f\rangle$ denote initial and final electronic states with electronic energies ε_i and ε_f, respectively. Further, $\hat{T}_{nuc}$ is the nuclear kinetic-energy operator which couples vibrational and electronic wave functions, and $\hbar\omega_{vu} = E_v - E_u$ is the energy difference between initial and final vibrational state. Under certain approximations, in particular (i) the assumption of separability of the coupling matrix element $|\langle v,i|\hat{T}_{nuc}|u,f\rangle|$ into nuclear and electronic parts and (ii) the harmonic approximation for vibrations, Eq. (1) implies simple selection and scaling laws for the vibrational relaxation process,

$$\Delta v = -1, \quad (2)$$

$$\Gamma_{v\to v-1} = v\Gamma_{1\to 0}. \quad (3)$$

According to Eq. (2), only stepwise single-phonon emission is possible, and according to Eq. (3) the decay rate of higher excited states increases linearly with the vibrational quantum number; $\Gamma_{1\to 0}^{-1}$ is the inverse vibrational lifetime τ_{vib} at $T=0$. Head-Gordon and Tully[9] developed a nonempirical molecular-orbital method to calculate vibrational lifetimes based on this approach and cluster models to represent the solid, which was recently extended to account for periodic boundary conditions.[10] A related approach for calculating lifetimes of vibrating adsorbates has been developed by Helssing and Persson.[11] In their work, a golden-rulelike expression is derived from density-functional theory (DFT), under approximations such as slowly varying electronic density and quasistatic limit. This method has been implemented[12] and applied to systems such as CO on copper and silver.[13] In these works, the authors take advantage of periodic DFT calculations which are known to be suitable for describing metal surfaces.

The perturbative Eq. (1) holds in the weak-coupling approximation, when electrons just below the Fermi level are excited to just above it. Closely related approaches were suggested to compute electronic friction coefficients, which can be used in classical, dissipative dynamics.[14] In these models, the transfer of translational or vibrational energy to metal electrons is included by means of a friction term in a Langevin equation. The method and simplified variants of it, have been used for atom-surface scattering,[15] molecule-surface scattering,[2,16] and hot-electron mediated photodesorption.[17–19]

Tully and co-workers recently suggested that single-quantum theories founded on (weak-coupling) perturbation theory cannot explain the strongly nonadiabatic behavior observed for NO($v\approx 15$)@Au(111).[20–23] Instead, they constructed a model Hamiltonian based on a Newns-Anderson model comprising a neutral ground-state NO/Au, an ionic state NO^-/Au^+, and a discretized metal continuum for electron-hole pair (EHP) excitations in the metal. Nonadiabatic dynamics were realized within a multistate 0 surface hopping scheme (IESH, independent electron surface hopping), which allows for multiple EHP creation. The IESH scheme also accounts for the observed, multiquanta relaxation of scattered NO, leading to a broad, relaxed vibrational energy distribution. In Ref. 22, it was argued, for NO($v=2$)@Au(111), that in contrast a classical friction model gives no broad vibrational energy distribution, despite the total energy loss was consistent with the IESH model.

In our own work, we aim at a quantum-mechanical treatment of inelastic scattering of NO(v) from Au(111), which fully accounts for quantized NO vibrations, wave-packet interference, and other quantum effects. This is missing at present. In principle, dissipative effective two-state models (which implicitly account for continua) or nondissipative multistate models (which explicitly account for continua) could be used for this purpose. This has been done, for example, for scattering of NO from metals,[24,25] and for hot-electron mediated photodesorption of NO from Pt(111) (Refs. 26–28) in the past. The quantum-mechanical modeling is very costly and was therefore restricted to the most important dynamical modes only, a strategy which we will follow here also.

The quantum multiple-state models have further, like their classical counterparts, the disadvantage that couplings between electronic states and/or electronic lifetimes of excited states are not known accurately and must often be adjusted empirically. Here we advocate a parameter-free model instead by combining quantum-mechanical open-system density-matrix theory with vibrational relaxation rates calculated from perturbative expressions such as Eq. (1). In that sense, and also because only a single electronic state is explicitly considered, our approach is of the electronic friction type. Thus, this paper addresses the importance and magnitude of electronic friction for NO@Au(111) within a fully quantum-mechanical treatment. It will be demonstrated, that the model accounts for vibrational state distributions which are compatible with experiment. The calculations of potentials and vibrational lifetimes are based on periodic DFT.

In our case, the coordinates that define the distance between the molecule and the surface and the internuclear distance constitute only two dimensions of a problem that, in principle, requires six dimensions. The intrinsic limitations of reduced dimensional models are well known: In the context of diatomic molecules interacting with metals, Refs. 3–5 and 29, for example, show, in the context of quantum dynamics, the importance of the dimensionality in order to achieve an accurate description of the scattering phenomena at surfaces. We believe however that the treatment of the most relevant coordinates permits us to address convincingly the importance of the electronic friction in this context.

The paper is organized as follows. In the next Sec. II, we describe the methods used here to calculate potentials, (coordinate-) dependent vibrational lifetimes, and the dissipative scattering dynamics. Results will be presented in Sec. III. A final Sec. IV concludes our work.

II. METHODS AND MODEL

A. Density-matrix model

The inelastic scattering of NO(v) from Au(111) will be modeled with the help of open-system density-matrix theory, using a two-mode model and a single electronic potential. The two selected modes are the vibrational coordinate, i.e., the N-O distance r, and the scattering coordinate Z, which is defined as the distance of the center-of-mass of NO to the closest Au atom in the surface layer. It is assumed that NO remains, like in its lowest-energy adsorbed state (see Sec. III A), in perpendicular orientation relative to the surface, with the N atom pointing toward it—cf. the inset of Fig. 1 below. This model neglects rotational and lateral motions of NO but has been shown to yield reasonable results for NO scattering[24] and photodesorption[27] from Pt(111).

In particular, the dynamical simulations are performed using the so-called coupled-channel density matrix (CCDM) method,[30,31] which is a tool for solving multidimensional Liouville-von Neumann equations. We apply this method to the propagation of the reduced density operator $\hat{\rho}(r,r',Z,Z')$ of the scatterer (the NO molecule), when coupled to a dissi-

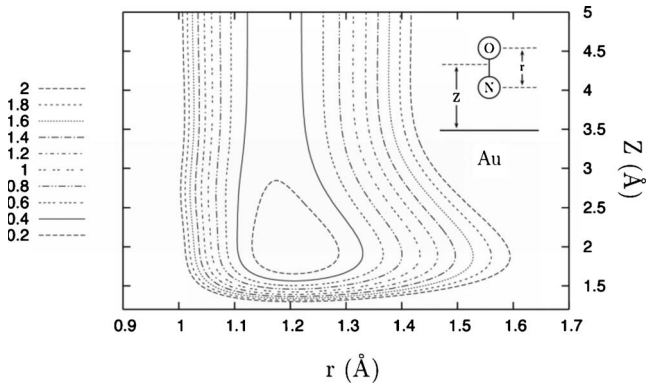

FIG. 1. Contour plot of the two-dimensional, fitted potential-energy surface $V(r,Z)$. Energy values are given in electron volt. The coordinates used are shown in the inset.

pative environment (the gold surface). The time evolution of the density operator is governed by the Liouville-von Neumann equation,

$$\frac{d\hat{\rho}(t)}{dt} = \mathcal{L}_H\hat{\rho}(t) + \mathcal{L}_D\hat{\rho}(t). \tag{4}$$

Here,

$$\mathcal{L}_H\hat{\rho} = -\frac{i}{\hbar}[\hat{H},\hat{\rho}(t)] \tag{5}$$

is the Hamiltonian Liouvillian, describing the unitary evolution of the isolated system under the influence of the system Hamiltonian,

$$\hat{H} = -\frac{\hbar^2}{2\mu_r}\frac{\partial^2}{\partial r^2} - \frac{\hbar^2}{2\mu_Z}\frac{\partial^2}{\partial Z^2} + V(r,Z) \tag{6}$$

with μ_r denoting the NO vibrational mass ($\mu_r = m_N m_O/m_{NO}$), μ_Z the scattering mass ($\mu_Z = m_{NO}$), and $V(r,Z)$ the ground-state potential. Further, $\mathcal{L}_D$ is the dissipative Liouvillian for which we adopt the Lindblad semigroup form[32]

$$\mathcal{L}_D\hat{\rho}(t) = \sum_{u,v} C_{u,v}\hat{\rho}C_{u,v}^{\dagger} - \frac{1}{2}[C_{u,v}^{\dagger}C_{u,v},\hat{\rho}]_+, \tag{7}$$

where $[\ ]_+$ is an anticommutator. The $C_{u,v}$ are Lindblad operators,[33]

$$C_{u,v} = \sqrt{\Gamma_{v\to u}(Z)}|u\rangle\langle v|, \tag{8}$$

which enforce electron-hole-pair-driven transitions from NO vibrational state $|v\rangle$ to state $|u\rangle$, with a damping rate $\Gamma_{v\to u}(Z)$ that depends on the molecule-surface distance. In particular, $\lim_{Z\to\infty}\Gamma_{v\to u}(Z)=0$ far from the surface, and $\Gamma_{v\to u}(Z)\neq 0$ closer to the surface where coupling to the electron-hole pair "bath" is efficient (see below).

In the CCDM method, one makes use of the fact that one mode (in our case r) is "bound" and can efficiently be represented in the basis of the vibrational eigenstates of NO while the other one (Z) is unbound and better represented on an equidistant grid. Thus, the two-dimensional (2D) density operator is expressed as

$$\hat{\rho}(Z,Z') = \sum_{u,v}^{K} \hat{\rho}_{u,v}(Z,Z')|u\rangle\langle v|, \tag{9}$$

where K is the number of vibrational basis functions (channels) used in the expansion, which is a convergence parameter of the CCDM scheme. The vibrational basis functions $\{|v\rangle\}$ are calculated as eigenfunctions of a one-dimensional reference Hamiltonian using the Fourier grid Hamiltonian method,[34]

$$\hat{H}_{ref}|v\rangle = E_v|v\rangle, \tag{10}$$

$$\hat{H}_{ref} = -\frac{\hbar^2}{2\mu_r}\frac{\partial^2}{\partial r^2} + V(r,Z_{ref}), \tag{11}$$

where Z_{ref} is a reference point, chosen as $Z_{ref}=4.5$ Å in the following. With this choice, the NO molecule is essentially decoupled from the surface, and the $\{|v\rangle\}$ describe correctly the asymptotic behavior of vibrational states of free NO. With the ansatz [Eq. (9)] used in Eq. (4) one obtains, in the mixed representation with N equidistantly chosen grid points along Z, $Z_r = Z_0 + (r-1)\Delta Z (r=1,\ldots,N)$, and K channels, the following expressions for the Hamiltonian and dissipative parts of the Liouvillian:[31]

$$[\mathcal{L}_H\hat{\rho}(t)]_{uv}^{rs} = -\frac{i}{\hbar}\Bigg[(E_u - E_v)\rho_{uv}^{rs} + \sum_{t=1}^{N}(T^{rt}\rho_{uv}^{ts} - \rho_{uv}^{rt}T^{ts}) + \sum_{w=0}^{K-1}(V_{uw}^{rr}\rho_{wv}^{rs} - \rho_{uw}^{rs}V_{wv}^{ss})\Bigg], \tag{12}$$

$$[\mathcal{L}_D\hat{\rho}(t)]_{uv}^{rs} = \sum_{w=0}^{K-1}\Bigg[\delta_{uv}\sqrt{\Gamma_{w\to u}^{rr}}\rho_{ww}^{rs}\sqrt{\Gamma_{w\to u}^{ss}} - \frac{1}{2}(\Gamma_{u\to w}^{rr} + \Gamma_{v\to w}^{ss})\rho_{uv}^{rs}\Bigg]. \tag{13}$$

The sum of the two gives the change in density-matrix element ρ_{uv}^{rs} in time. In the above equations, the general notion $O_{uv}^{rs} = \langle r|\langle u|\hat{O}|v\rangle|s\rangle$, has been used, where upper indices r, s, and t are grid point, and lower indices u, v, and w are vibrational state indices. The inner integration is over the r and the outer over the Z coordinate. Further, $T^{rt} = \langle r|-\frac{\hbar^2}{2\mu_Z}\frac{\partial^2}{\partial Z^2}|t\rangle$ is a matrix element of the kinetic-energy operator for motion along Z, which is evaluated by fast Fourier transform techniques below.[30] Further, each of the K vibrational states is characterized by a one-dimensional potential $V_{vv}(Z) = \langle v|V(r,Z) - V(r,Z_{ref})|v\rangle$, which is coupled through potential terms,

$$V_{uv}^{tt} = \langle u|V(r,Z_t) - V(r,Z_{ref})|v\rangle \tag{14}$$

to other vibrational states $|u\rangle$ at point Z_t.

According to Eq. (13), the different vibrational states are also coupled through coordinate-dependent quenching rates $\Gamma_{u\to v}^{rr} = \Gamma_{u\to v}(Z_r)$ as required. Note that, in principle, also the translational mode can couple to EHP, which is neglected in Eq. (13). This approximation is reasonable, since, in contrast to the NO stretching mode, the relaxation time of the

molecule-surface mode is considerably longer than typical "contact times" of the scattering NO with the surface (see below). Vibration-phonon coupling is also neglected for the same reason.

The CCDM method is efficient if the number of channels K is small as compared to the number of grid points which would be needed to represent the bound coordinate. This is usually the case. One then propagates K coupled density-matrix blocks of size $N \times N$ each, instead of a single density matrix of size $(N_r \cdot N_Z) \times (N_r \cdot N_Z)$.

In practice, we start with a density operator corresponding to a NO molecule in vibrational state $|v_{in}\rangle$ described as a Gaussian wave packet of width σ, centered initially around $Z=Z_\infty$, and approaching the surface with mean momentum $\hbar k_{0Z}$,

$$\hat{\rho}(0) = |v_{in}\rangle\langle v_{in}| \otimes |Z\rangle\langle Z'|g(Z)g^*(Z'), \tag{15}$$

$$g(Z) = \frac{1}{(2\pi\sigma^2)^{1/4}} \exp\left\{ ik_{0Z}Z - \frac{(Z-Z_\infty)^2}{4\sigma^2} \right\}. \tag{16}$$

This corresponds to an initial mean kinetic energy of $E_k = \frac{\hbar^2 k_{0Z}^2}{2\mu_Z}$. Below we chose $\sigma=0.5$ Å, $Z_\infty=5$ Å, and different kinetic energies and initial vibrational states. In all cases, $K=22$ channels were included in the calculation, and the number of Z-grid points was $N=256$, starting from $Z_0=1.13$ Å with a grid spacing $\Delta Z=0.027$ Å. The nonsparse density matrix thus contains 5632×5632 elements. The time propagation of the density operator in Eq. (4) was done on a time grid with a Newton polynomial propagator[26,35] of order 16, and a time step of $\Delta t=0.25$ fs.

Observables are calculated from the trace relation $\langle \hat{O} \rangle = \mathrm{tr}\{\hat{\rho}(t)\hat{O}\}$. In particular, vibrational state populations are determined as

$$P_v(t) = \mathrm{tr}\{\hat{\rho}(t)|v\rangle\langle v|\}. \tag{17}$$

B. DFT calculations for adsorption geometries and ground-state potential

Periodic density-functional calculations based on Kohn-Sham theory[36] were performed with the plane-wave-based VASP code,[37,38] using the PW91 exchange-correlation functional,[39] to obtain stable adsorption sites of NO on Au(111), and to calculate the potential-energy surface $V(r,Z)$.

When searching for adsorption sites, the substrate is represented by a $3 \times 3 \times 6$ periodically repeated cell (six-layer slab, each layer containing nine atoms), and the vacuum spacing perpendicular to the surface between each periodically repeated unit cell is 1.2 nm. Per cell, a single NO molecule was considered which corresponds to a coverage of 1/9. The reciprocal space was described by a $7 \times 7 \times 1$ Monkhorst-Pack grid,[40] and the energy cutoff was set to 500 eV. During adsorption site search, ionic relaxation was performed. Here, three top layer atoms were free to move as well as the atoms of the adsorbate, their coordinates changed until a force of 0.01 eV/Å or less was reached. The calculations were all spin polarized because NO is an open-shell molecule.

When calculating the potential surface $V(r,Z)$, a reoptimization of the first-layer ion cores was performed. Around 60 points were computed in this case using the same supercell but only with three atom layers, to lower the computational cost of this task. The changes in the relevant distances between the equilibrium geometries of the six-layer slab, and the three-layer slab, the N-O distance and the adsorption distance, varied by less than 1%.

C. Vibrations and vibrational damping rates

After the relaxation of the ions, a normal-mode analysis (NMA) was performed to obtain the harmonic frequencies ω_λ of the mode λ and the eigenvectors of the dynamical (Hessian) matrix, i.e., the normal modes $\underline{R}_\lambda$. This calculation essentially consists in computing energy derivatives with respect to coordinates by centered finite differences. The displacements are done two times in the three directions of space for each active atom and, as we restricted the number of active atoms to 11 for computational reasons (only the atoms of the molecule and the ones in the first layer of the slab were included), $11 \times 3 \times 2 = 66$ calculations were necessary. Including the atoms of the metal is reasonable because close to the surface, the vibrations of the molecule can perturb the gold atoms. Out of all normal modes, only those corresponding to the two modes in our reduced-dimensional model, r and Z will be considered in greater detail below.

In order to compute the lifetime of these two modes in the equilibrium configuration, we proceed along the lines of Fermi's golden rule. Within the "periodic DFT route" advocated in Ref. 12, the fundamental deexcitation rate of mode λ can be approximated, when generalized to finite temperature, as

$$\Gamma^\lambda_{1\to 0} = \frac{2\pi}{\hbar} \sum_{n,m,\underline{k}} \left| \langle 1, n\underline{k} | \frac{\partial \hat{H}_{el}}{\partial \underline{R}_\lambda} \delta \underline{R}_\lambda | 0, m\underline{k} \rangle \right|^2 f_n[1-f_m] \times \delta(\varepsilon_{n,\underline{k}} - \varepsilon_{m,\underline{k}} + \hbar\omega_\lambda). \tag{18}$$

This expression is written using Bloch states, which is a natural basis when dealing with periodically repeated cells: n and m are the band indexes, $\underline{k}$ is a wave vector in the Brillouin zone, and f_n and f_m are the Fermi functions that ensure that n is an occupied state, and m an empty one. All the calculations presented in this work have been made at $T=0$. The term $\delta(\varepsilon_{n,\underline{k}} - \varepsilon_{m,\underline{k}} + \hbar\omega_\lambda)$ accounts for the conservation of total energy as above, with $\varepsilon_{m,\underline{k}}$ denoting the single-particle energy of band m and k-point $\underline{k}$. In practice, we use periodic, gradient-corrected DFT also here which means that $\varepsilon_{m,\underline{k}}$ are Kohn-Sham energies. Further, $\partial \hat{H}_{el}/\partial \underline{R}_\lambda$ are first derivatives of the electronic Hamiltonian $\hat{H}_{el}$, taken at the equilibrium position $\underline{R}^0_\lambda$. Finally, $\delta \underline{R}_\lambda = \underline{R}_+ - \underline{R}_-$ is the displacement of coordinate λ around the equilibrium position because we use centered finite differences. We employ harmonic oscillator eigenfunctions to represent the vibrational part of the wave function because this is a equilibrium situation. If we separate electronic and vibrational parts in Eq. (18), one can write,

$$\Gamma^{\lambda}_{1\to 0} = \frac{2\pi}{\hbar}\sum_{n,m,\underline{k}} \left| \langle n\underline{k}| \frac{\partial \hat{H}}{\partial \underline{R}_{\lambda}} |m\underline{k}\rangle \right|^2 |\langle 1|\delta \underline{R}_{\lambda}|0\rangle|^2 f_n[1-f_m] \times \delta(\varepsilon_{n,\underline{k}} - \varepsilon_{m,\underline{k}} + \hbar\omega_{\lambda}). \quad (19)$$

The vibrational part of the expression (19) can be calculated analytically using the usual relation for the harmonic oscillator, $\langle 1|\delta \underline{R}_{\lambda}|0\rangle = \sqrt{\frac{\hbar}{2\mu_{\lambda}\omega_{\lambda}}}$. Note that in this harmonic approximation with linear coupling, a generalization of Eq. (19) to arbitrary $v \to u$ transitions fulfills automatically the selection/scaling laws (2) and (3). The electronic matrix element $|\langle n\underline{k}|\frac{\partial \hat{H}_{el}}{\partial \underline{R}_{\lambda}}|m\underline{k}\rangle|$ was calculated with finite differences displacing the atoms along the normal modes. In practice, this implies the use of the eigenstates $|m\underline{k}\rangle_{\pm}$ and their corresponding eigenvalues.

In the work by Lorente and Ueba,[13] a careful study was performed for CO on copper and silver. The authors point out that the k-point sampling is a critical issue. We want to stress that all lifetime calculations were performed using a k-point $7\times 7\times 1$ grid in order to have reliable results.[10,13] Another important technical point is that the delta function in Eq. (19) has been approximated by a Gaussian,

$$\delta(\varepsilon_{n,\underline{k}} - \varepsilon_{m,\underline{k}} + \hbar\omega_{\lambda}) \approx \frac{1}{\sqrt{\pi a^2}} e^{-(\varepsilon_{n,\underline{k}} - \varepsilon_{m,\underline{k}} + \hbar\omega_{\lambda})^2/a^2}. \quad (20)$$

This is only true in the limit where the width parameter a tends to zero but here because of the discrete representation of the reciprocal space, a has to be nonzero. Calculations have been performed to check the behavior of the damping rates with the width of the Gaussian distribution and we found a linear behavior around $a=0.12$ eV for both modes, a value which was adopted below.

For the CCDM equations, coordinate-dependent damping rates $\Gamma_{u\to v}(Z)$ for arbitrary v and u are needed. For those we adopt in the spirit of the harmonic-linear approximation, the simple selection and scaling relations (2) and (3), and we calculate $\Gamma_{v\to v-1}(Z) = v\Gamma_{1\to 0}(Z)$ for every Z-point separately, using Eq. (19) and $\underline{R}_{\lambda=r}$. Further, the quantity $\langle 1|\delta r|0\rangle$ in Eq. (19) was calculated by simple integration over the r coordinate, where $|1\rangle$ and $|0\rangle$ are anharmonic, one-dimensional vibrational eigenstates $|v\rangle$ determined from Eq. (10), with Z_{ref} being replaced by the particular point Z of interest. Note that when using these anharmonic vibrational wave functions and Eq. (19), one could in principle also calculate anharmonic decay rates $\Gamma_{v\to u}(Z)$ for any combination v and u directly, which will lead to a deviation from the simple laws (2) and (3).

The electronic part of Eq. (19) was treated using finite differences as before. To calculate the different matrix elements, we used a displacement along the r coordinate proportional to the previously calculated $\langle 1|\delta r|0\rangle$ in order to simplify the implemented expression for the damping rates.

III. RESULTS

A. Adsorption site and potential-energy surface

Using the DFT protocol as outlined in Sec. II B, the minimum-energy configuration of NO/Au(111) was obtained when adsorbing the NO molecule on a fcc site, the molecular axis being perpendicular to the surface and the nitrogen pointing toward it. The adsorption energy for this configuration was 340 meV. Systematic calculations showed that other local minima exist, however they give lower adsorption energies. In particular, when the molecules sits in the hcp site, the binding energy was 280 meV. We find that the equilibrium N-O distance is $r_{eq}=1.194$ Å and the distance of the molecule's center of mass to the nearest Au atom is $Z_{eq}=2.08$ Å, i.e., the nitrogen atom lies at $Z_N=1.73$ Å above the surface. These values are in strong agreement with the work of Roy *et al.*,[22] who find $r_{eq}=1.192$ Å and $Z_N=1.60$ Å or 1.82 Å depending on whether they consider directly the computed data, or their analytic fit to the computed potential-energy surface. In the present work, the positions of the atoms of the first layer were fully relaxed when fixing r,Z to determine one of the points of the potential-energy surface.

Although our calculated adsorption energies are higher than in previous works,[22,41] we confirm that the fcc adsorption site is the preferred one. The potential-energy surface $V(r,Z)$ was calculated along the lines described in Sec. II B, in the interval $r\in[0.98,1.60]$ and $Z\in[1.6,4.5]$. For dynamics, an analytic fit to the calculated ($\approx$60, see above) points was made without any restriction in r or Z, using a rational function, essentially given by two coupled Morse potentials. For fitting, the standard nonlinear least-squares Marquardt-Levenberg algorithm[42] was used. Since the two degrees of freedom considered are coupled, we introduced couplings between the two Morse potentials. This was achieved by replacing the usual parameters of the Morse potential by switching functions[43] depending in turn on a new set of parameters, which are adjusted by the fitting procedure. Here we adopted a simple from of the switching function,

$$S_{(\pm)}(q;n,q_0) = \frac{1}{2}\{1 \pm \tanh[n(q-q_0)]\}, \quad (21)$$

where the symbol $\pm$ stands for a function either rising from 0 to 1 or falling from 1 to 0. q is a general coordinate and n and q_0 are the switching parameters, n is related to the steepness of the increase/decrease in the function and q_0 is the value of the coordinate where the switching occurs, i.e., $S_{(\pm)}(q_0;n,q_0)=\frac{1}{2}$. The precise form of the fitting function $V(r,Z)$ is given in the Appendix.

In Fig. 1, a contour plot of the fitted potential-energy surface is presented. For values of Z larger than about 3.5 Å, the potential along the stretch coordinate r remains the same because the molecule does no longer interact with the surface strongly. For distances smaller than $Z=3.5$ Å, the Morse potential along r is considerably softened due to proximity of the surface. The minimum of $V(r,Z)$ almost quantitatively reproduces the equilibrium position and adsorption energy found by geometry optimization.

During the adsorption process, the unpaired spin of the approaching molecule is quenched as demonstrated in Fig. 2(a). There, the computed spin polarization $N_{\alpha}-N_{\beta}$ (difference of the number of α and β electrons) is shown as a function of Z, with r fixed at its (adsorption) equilibrium

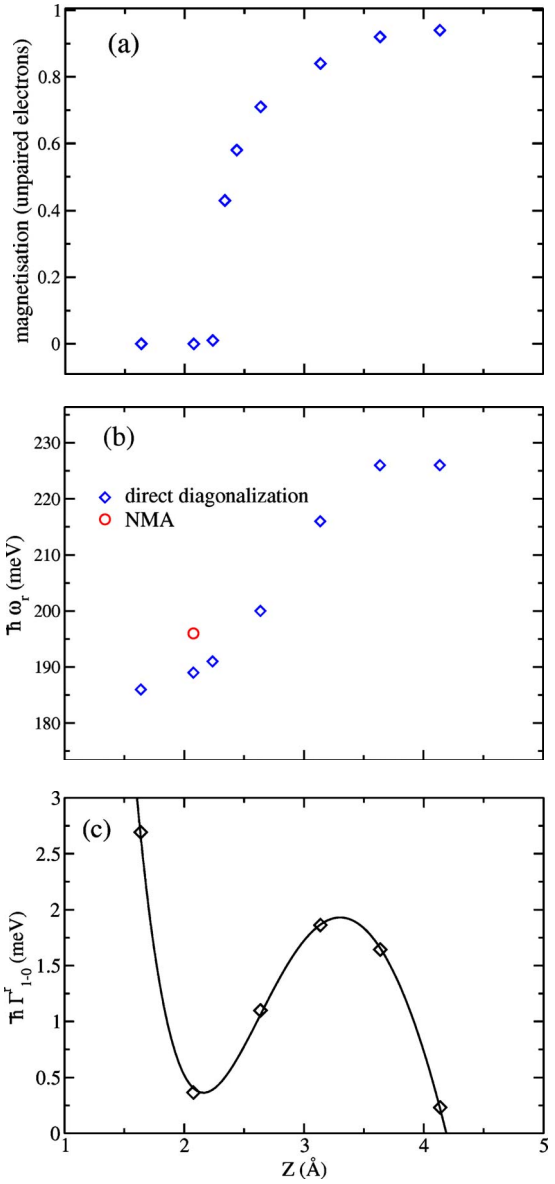

FIG. 2. (Color online) Computed properties as a function of NO-surface distance Z. (a) Magnetization; (b) vibrational frequencies of N-O stretch mode obtained from diagonalizing Eq. (11) (diamonds) or NMA at the adsorption geometry (circle); (c) vibrational damping widths $\hbar\Gamma^r_{1\to 0}$ (diamonds) and a fifth-order polynomial fit to it (solid line): $f(Z)=\Sigma_{n=0}^{5}A_nZ^n$, with parameters $A_0=123.21$ meV, $A_1=-186.12$ meV Å^{-1}, $A_2=107.92$ meV Å^{-2}, $A_3=-30.044$ meV Å^{-3}, $A_4=4.0805$ meV Å^{-4}, and $A_5=-0.22123$ meV Å^{-5}.

value. It is seen that the polarization drops rapidly from one to zero when approaching the surface. At around $Z\approx 2.5$ Å, the value is 1/2 and practically zero at around the adsorption bond length of $Z_{eq}=2.08$ Å.

B. Vibrations and vibrational damping rates

1. Adsorbed species

As stated in Sec. II C, in order to describe the dissipative nature of the problem coordinate-dependent damping rates are needed. First of all let us consider the NO molecule when adsorbed on top of Au in its equilibrium position. For this stationary point, a normal-mode analysis has been carried out as described in Sec. II B. Two of the computed normal modes reflect, in excellent approximation, the N-O stretch mode (r) and the NO-surface mode (Z), respectively, with very little admixture of other atom motions. The fundamental energy $\hbar\omega_r$ of the N-O stretch mode is 196 meV and the one of the NO-surface stretch mode, $\hbar\omega_Z$, is 22 meV (see Table I).

TABLE I. Harmonic frequencies and vibrational width and lifetime parameters of NO adsorbed in on-top position on Au(111).

	N-O stretch ($\lambda=r$)	NO-surface ($\lambda=Z$)
$\hbar\omega_\lambda$ (meV)	196	22
$\hbar\Gamma^\lambda_{1\to 0}$ (meV)	0.365	0.061
τ^λ_{vib} (ps)	1.8	7.3

For the adsorbed species, the damping rate was calculated with the help of Eq. (19), using the techniques described in Sec. II C. The energy width $\hbar\Gamma^\lambda_{1\to 0}$ associated with a finite damping rate, was 0.365 meV for $\lambda=r$, which corresponds to a lifetime $\tau^r_{vib}=1/\Gamma^r_{1\to 0}$ of approximately 1.8 ps for the N-O stretch mode. The corresponding values for the NO-surface vibration are $\hbar\Gamma^Z_{1\to 0}=0.089$ meV and $\tau^Z_{vib}=7.3$ ps. These values are typical when dealing with diatomic molecules on metal surfaces: The C-O stretch mode on Cu(110) has a damping width of 0.30 meV and for the CO-surface mode a value of 0.061 meV has been found by Lorente *et al.* in a similar calculation.[13] For NO/Pt(111), $\tau^r_{vib}=8.2$ ps and $\tau^Z_{vib}=9.6$ ps were calculated in Ref. 10 by a slightly different approach.

2. Z-dependent NO stretching frequencies and lifetimes

A series of calculations yields the frequency and the damping rate of the N-O stretch vibration as a function of Z as outlined in Sec. II C. We remind the reader that now the NO vibrational states were calculated anharmonically from one-dimensional cuts through the 2D surface [cf. Eqs. (10) and (11)], which were then used in Eq. (19). Of course, this can only be an approximation since r and Z modes are not strictly separated in the 2D model.

In Fig. 2(b), we present the results of the frequencies of the stretch-mode N-O as a function of the NO-surface distance Z. Far from the surface the frequency is constant, $\hbar\omega_r=226$ meV. This reflects reasonably well the experimental gas phase value of 236 meV for free NO.[44] Closer to the surface, the potential softens along r (see Fig. 1), resulting in smaller vibrational frequencies. According to Fig. 2(b), the frequency at around the equilibrium position Z_{eq} is 189 meV. The value from normal mode analysis [circle in Fig. 2(b)], is thus 7 meV larger.

In Fig. 2(c), the damping rates are presented as a function of the coordinate Z. The dots are our calculations and the curve is a fifth-order polynomial fitted to the points using a standard least-squares fitting. At the equilibrium position Z_{eq}(2.08 Å), the width parameter $\hbar\Gamma^r_{1\to 0}$ is 0.365 meV, in

perfect agreement with the results from the NMA (see Table I). As expected, closer to the surface the damping rate rises due to strong interaction with the metal electrons At $Z=1.64$ Å, for example, the width is 2.69 meV, corresponding to a vibrational lifetime of about 250 fs. One would expect a monotonically decreasing behavior of $\hbar\Gamma^r_{1\to 0}$ for increasing Z but this not the case. Instead one finds a local maximum around $Z=3.3$ Å, corresponding to a lifetime of about 350 fs. For larger Z, the damping width decreases rapidly again. The nonmonotonic behavior is an effect due to the spin transition which takes place in the region of the local rate maximum, see Fig. 2(a) and the discussion in Sec. III A. A similar spin quenching effect has already been described in the case of hydrogen on Cu(111) by Trail *et al.*[45] In a later work,[46] these authors show that due to broadening and shifting of the involved electronic levels of H, the spin loss leads to a significant increase in the friction coefficient in the region where the transition occurs. We believe that our calculations show the same behavior as in H/Cu(111) because the nitric oxide is an open-shell molecule as well.

The fifth-order polynomial fit given in Fig. 2(c) is unphysical in the sense that it abruptly drops to zero at around 4.2 Å, rather than smoothly decaying. Still, we use the analytic fit for the dynamics calculations below because differences in detail at large Z, where the damping rates are very small, are dynamically irrelevant.

C. Dissipative dynamics

To simulate the scattering of highly vibrationally excited NO molecules, excited Gaussian wave packets are prepared according to Eqs. (15) and (16), with the choices $v_{in}=15$ and 14. Two different kinetic energies $E_k=0.3$ eV and $E_k=0.6$ eV were chosen. The experimental value of $E_k=0.05$ eV (Ref. 6) cannot be reached at the moment since low kinetic energies require prohibitively large grids.

As the wave packet propagates toward the surface, population is transferred from the v_{in} level to lower vibrational levels by the Z-dependent transition rates, $\Gamma^r_{v\to u}(Z)$. Other states are also accessible through potential coupling, i.e., transfer of energy from the r to the Z mode, however, dissipation dominates. In the harmonic damping model, the scaling law given in Eq. (3) is followed and according to Eq. (2), vibrational energy can only be transferred from a level to its nearest downward neighbor. Note that because of Eq. (3), the lifetime of highly vibrationally excited NO molecules can be very short close to the surface. For example, the transition time to the next lowest level at around $Z_{eq}=2.08$ Å drops from 1.8 ps for $v=1$, to about 120 fs for $v=15$.

Figure 3 shows the evolution of the population of selected vibrational levels as a function of time. The initial kinetic energy was set to 0.6 eV in this case, and $v_{in}=15$. After the wave packet has reached the high-damping region, the population of the 15th state shows a significant decrease during the first 100 fs, accompanied by a sequential increase in population of lower-v states. This behavior is essentially given by the fact that in our model, the population transfer is stepwise as previously stated. Closer inspection reveals that the population of the 15th state shows a particular behavior.

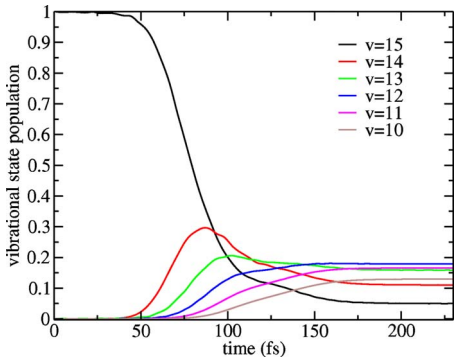

FIG. 3. (Color online) Population analysis as a function of time. The 15th vibrational level is occupied at $t=0$, initial translational energy is 0.6 eV.

A particularly rapid decrease is observed twice, at around 70 fs and at around 130 fs. We attribute this to the fact that the initial wave packet explores two times the region around $Z=3.3$ Å where the damping rates are high, one time when approaching the surface, and again after scattering. Note that this behavior is reflected as well by two subsequent increases in population of lower vibrational levels. After the final propagation time of $t=236$ fs, the asymptotic region is reached and changes in all populations no longer occur.

An analysis of the asymptotic populations is done in Fig. 4(a). It is clearly seen that the major part of the population has been transferred to lower vibrational levels. A maximum at $v=12$ occurs, and the final vibrational state distribution is broad: States $v=8$ to $v=15$ all carry populations of about 0.05 or larger. Also states with $v>15$ carry some small amount of population (not shown), which is due to the fact that even without dissipation the vibrational state distribution broadens by vibration-translation coupling. The latter fact is

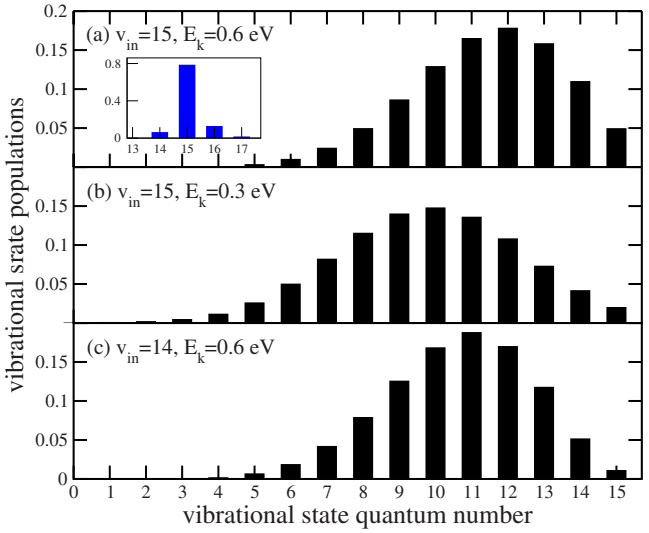

FIG. 4. (Color online) Asymptotic vibrational state populations for scattered NO(v) molecules. (a) For initial vibrational state $v_{in}=15$ and initial kinetic energy $E_k=0.6$ eV, (b) $v_{in}=15$ and $E_k=0.3$ eV, (c) $v_{in}=14$ and $E_k=0.6$ eV. The inset to (a) shows non-negligible final state populations for the dissipation-free case and $v_{in}=15$, $E_k=0.6$ eV.

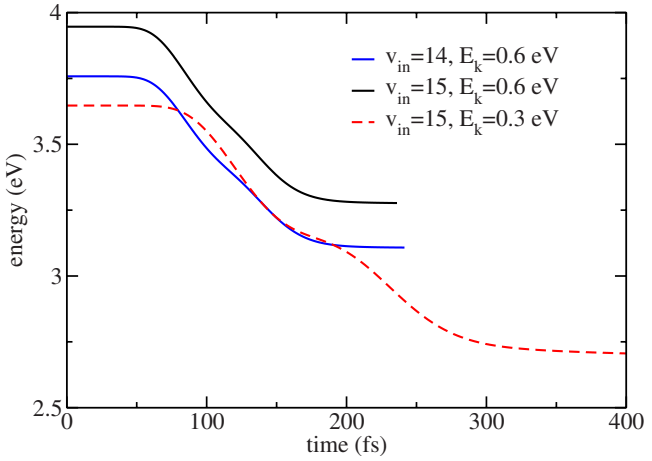

FIG. 5. (Color online) Energy loss as a function of time. The different curves correspond to different values of initial vibrational state and kinetic energy. Due to the low kinetic energy used to calculate the red dashed curve, the final propagation time had to be extended to t_f=400 fs in order to reach the asymptotic limit.

demonstrated in the inset of Fig. 4(a), which shows the dissipation-free case with nonvanishing populations not only for $v=15$ but also for $v=16$, $v=17$, and $v=14$.

The black curve in Fig. 5 shows the system energy during the scattering event for the same initial conditions (i.e., initial vibrational state $v_{in}=15$ and $E_k=0.6$ eV). For dissipative dynamics, the system energy, calculated as $E=\mathrm{tr}\{\hat{\rho}\hat{H}\}$ is not conserved. It is seen again that after the total propagation time of 236 fs the scattering process is over, and the energy dropped from 3.95 eV to about 3.28 eV. Thus, about 0.67 eV of energy has been transferred to the substrate during this time. Here, the initial energy defined as the initial vibrational energy of the molecule (3.35 eV including zero-point energy) plus the translational energy. The energy difference between the 15th and the 12th vibrational state of free NO, when calculated with our potential, is 0.58 eV which shows that in average about three vibrational quanta were lost, consistent with the vibrational state distribution in Fig. 4(a). Closer inspection of the black curve in Fig. 5 shows again two phases with slightly accelerated dissipation, reflecting the incoming and outgoing molecule passing through the enhanced-damping region around $Z=3.3$ Å.

In Figs. 4 and 5, we also study the effect of initial vibrational state and translational energy. In Figs. 4(c) and 5, blue curve (starting at 3.75 ev at $t=0$ fs), the lower initial state $v_{in}=14$ is considered while retaining $E_k=0.6$ eV, and in Figs. 4(b) and 5, red dashed curve, the effect of lower kinetic energies is tested by choosing $v_{in}=15$ and $E_k=0.3$ eV. Considering Figs. 4(a) and 4(c) we note that the effect of initial vibrational state is merely to shift the final vibrational state distribution by about one quantum to lower vibrational states. Figure 5, blue curve, shows in fact that the energy loss curves for $v_{in}=15$ and $v_{in}=14$ run almost parallel (their initial energy difference of 0.19 eV corresponds to $\hbar\omega_{15,14}$ of free NO), and the final energy loss is only slightly lower for $v_{in}=14$ than for $v_{in}=15$ (0.65 vs 0.67 eV). For much lower initial vibrational quantum numbers v_{in}, on the other hand, the energy loss is smaller in particular because the relaxation rates become smaller according to Eq. (3) (not shown).

TABLE II. Parameters calculated for the fitting function $V(r,Z)$.

Parameter	Value
D_0	4.65231 eV
D_{inf}	10.427 eV
a_0	2.62512 Å^{-1}
a_{inf}	2.08049 Å^{-1}
r_0	1.20697 Å
r_{inf}	1.16908 Å
D_u	0.28756 eV
a_u	1.94118 Å^{-1}
Z_u	1.96264 Å
Z_D	3.12897 Å
n_D	1.28184 Å^{-1}
Z_a	3.302 Å
n_a	1.00096 Å^{-1}
Z_r	2.40656 Å
n_r	1.99576 Å^{-1}

The effect of initial kinetic energy, however, is always large. This is demonstrated in Fig. 4(b), where we see a further broadened final vibrational state distribution when going from $E_k=0.6$ eV to $E_k=0.3$ eV. Also, the maximum of the final-state distribution is now at around $v=10$, which corresponds to an average loss of about five vibrational quanta during scattering. The energy difference between the 15th and 10th vibrational states of free NO is $\hbar\omega_{15,10}=0.97$ eV according to our potential. This fits well to the calculated energy loss reported in Fig. 5 (red dashed curve), which is 0.95 eV after $t=400$ fs. Note that the time period of the propagation is in this case longer than in the cases where the kinetic energy was higher. The final propagation time had to be extended in order to reach the asymptotic limit. For the same reason, the prolonged relaxation period at lower kinetic energies is a simple consequence of the longer contact time of the slower NO molecule with the surface.

In the experiment by Huang *et al.*,[6] the authors see a broad distribution of final vibrational populations, with a maximum around $v=7-8$. This corresponds to a loss of 7–8 vibrational quanta when starting from $v=15$. Assuming that other energy redistribution channels can be neglected, this corresponds to an energy loss of about 1.5 eV to the surface. (The energy differences $\hbar\omega_{15,7}$ and $\hbar\omega_{15,8}$ are 1.59 eV and 1.38 eV, respectively.) The experiments in Ref. 6 were done at an initial kinetic energy of $E_k=0.05$ eV as stated earlier. The relaxation is a complicated, multiexponential decay process. However, according to Fig. 5, it can be roughly idealized as an effective damping process, in which the energy decreases about linearly during a contact time, t_c. This can be used to estimate the energy loss at low initial kinetic energies. According to this simple model, the energy loss is $\Delta E \approx Rt_c$ where R is the energy damping rate. From Fig. 5, we estimate for $v_{in}=15$ and $E_k=0.6$ eV, $t_c\approx 150$ fs and $R \approx 0.67/150$ eV/fs≈ 4.5 meV/fs. Assuming that (i) the en-

ergy damping rate is approximately constant for a given v_{in}, and (ii) that, if the potential well is neglected, the velocity of the incoming NO is $v=\sqrt{2E_k/m_{\mathrm{NO}}}\propto 1/t_c$, the ratio of energy losses for two different initial kinetic energies is given by

$$\frac{\Delta E_1}{\Delta E_2} \approx \sqrt{\frac{E_{k,2}}{E_{k,1}}}. \tag{22}$$

From this last equation, we estimate with $E_{k,1}=0.6$ eV and $E_{k,2}=0.05$ eV, an energy loss of about $\Delta E_2 \approx 0.67\sqrt{0.6/0.05}$ eV$=2.3$ eV at the experimental impact energy. Clearly, this analysis is grossly oversimplified but it demonstrates, that substantial amounts of vibrational energy can be dissipated into the solid within the quantum-mechanical version of the electronic friction scenario. The quantum-mechanical friction model also accounts for a broad vibrational population distribution, similar to the one observed in experiment.[6]

IV. SUMMARY AND CONCLUSION

We have studied the vibrational relaxation of a highly vibrationally excited NO molecules scattering off a gold surface by means of the open-system density-matrix formalism, which allows for dissipative energy transfer from the molecule to the EHP continuum of the metal. Prior to our dynamical calculations, we used density functional theory to determine by geometry optimization the relevant quantities of the adsorbed system such as adsorption energies and vibrational lifetimes. The lifetimes were extracted from a Fermi golden rule expression involving the coupling of the vibrations of NO with the electronic degrees of freedom of the metal. Computed vibrational lifetimes are in the order of 2 ps for the N-O stretch mode of the adsorbed molecule, and about 7 ps for the NO-surface vibration. These two coordinates were also used to set up a two-dimensional potential-energy surface for dynamics. Coordinate-dependent damping rates were computed as well. The N-O vibrational damping rate shows an interesting spatial variation, with increased damping rates (shorter lifetimes) at NO-surface distances where the electron spin of NO is quenched during adsorption. Finally, the Liouville-von Neumann equation was solved in the coupled channel density-matrix formalism in a mixed representation.

It has been shown that our quantum-mechanical version of the electronic friction model, which allows only for stepwise relaxation along the vibrational ladder, can account for experimental facts found for NO($v=15$) scattering from Au(111): (i) substantial vibrational energy losses in the order of electron volts and (ii) a broad distribution of final-state populations. It has further been demonstrated that the nontrivial coordinate dependence of damping has subtle consequences for the dynamics.

Within the harmonic electronic friction model, multiquantum relaxation is a consequence of several, consecutive single-quantum transitions. These can occur, however, because the transition rates $\Gamma_{v\to v-1}$ for large v are in the order of 100 fs and below (depending on the molecule-surface distance), which is in the order of magnitude or shorter than, typical molecule-surface contact times. This explains also the broad vibrational state distribution of the scattered molecules. Thus, to explain the multiquantum energy loss and broad final-state distributions, we believe that electronic friction models are fully sufficient. However, in the friction model only low-energy electron-hole pairs are created because in a single energy transfer process, only one vibrational quantum needs to be absorbed at a time by the metal. This is fundamentally different from the electronic multistate models,[23] which allow for direct multiquantum relaxation and high-energy EHP creation, and thus, for electron emission from low-work function materials. It may very well be that these direct multiquantum relaxation processes and *explicit* multistate models to explain them, are needed in order to account for all experimental facts known for nonadiabatic molecule-surface scattering. We note, however, that in an anharmonic version of Fermi's golden rule to treat non-Born-Oppenheimer couplings, and/or when going beyond the linear-coupling approximation [see Eq. (19)], direct multiquantum relaxation becomes possible also in electron friction models. Their contribution is usually small, however, and it remains to be seen if they can make a significant contribution to NO scattering from Au(111). The inclusion of anharmonicities and nonlinearities leads also to smaller relaxation rates for high-v states than predicted by Eq. (3),[47] which may explain why the present friction model actually seems to lead to stronger dissipation than needed (cf. results of the simple extrapolation scheme of Sec. III C). We are also fully aware of the fact that our model can be improved in many other directions, most notably by including molecular rotations in order to make quantitative comparisons with experimental data possible.

ACKNOWLEDGMENTS

The authors thank Nicolás Lorente (CIN2 and ICN, Bellaterra, Spain) for fruitful discussions. Financial support by the Deutsche Forschungsgemeinschaft through project Sa 547/8-1 is gratefully acknowledged. Computational resources were provided by the Konrad-Zuse-Zentrum für Informationstechnik Berlin (ZIB).

APPENDIX: ANALYTICAL FIT OF THE POTENTIAL-ENERGY SURFACE

Here we give the functional form of the function fitting the first-principles data explicitly using the switching functions discussed in Sec. III A,

$$V(r,Z) = D_u\{1-\exp[-a_u(Z-Z_u)]\}^2 + \left[\frac{1}{2}D_0\{1-\tanh[n_D(Z-Z_D)]\} + \frac{1}{2}D_{inf}\{1+\tanh[n_D(Z-Z_D)]\}\right] \times\left\{1-\exp\left[-\left(\frac{1}{2}a_0\{1-\tanh[n_a(Z-Z_a)]\} + \frac{1}{2}a_{inf}\{1+\tanh[n_a(Z-Z_a)]\}\right)\left(r-\left(\frac{1}{2}r_0\{1-\tanh[n_r(Z-Z_r)]\} + \frac{1}{2}r_{inf}\{1+\tanh[n_r(Z-Z_r)]\}\right)\right)\right]\right\}^2. \quad \text{(A1)}$$

The parameters are given in Table II.

[1] M. Born and J. Oppenheimer, Ann. Phys. **84**, 457 (1927).
[2] J. I. Juaristi, M. Alducin, R. Diez Muino, H. F. Busnengo, and A. Salin, Phys. Rev. Lett. **100**, 116102 (2008).
[3] A. Gross, S. Wilke, and M. Scheffler, Phys. Rev. Lett. **75**, 2718 (1995); A. Gross, Surf. Sci. Rep. **32**, 291 (1998).
[4] P. Nieto, E. Pijper, D. Barredo, G. Laurent, R. A. Olsen, E.-J. Baerends, G.-J. Kroes, and D. Farias, Science **312**, 86 (2006).
[5] G.-J. Kroes, Prog. Surf. Sci. **60**, 1 (1999).
[6] H. Huang, C. Rettner, D. Auerbach, and A. Wodtke, Science **290**, 111 (2000).
[7] J. D. White, J. Chen, D. Matsiev, D. J. Auerbach, and A. M. Wodtke, Nature (London) **433**, 503 (2005).
[8] M. Morin, N. J. Levinos, and A. L. Harris, J. Chem. Phys. **96**, 3950 (1992).
[9] M. Head-Gordon and J. C. Tully, J. Chem. Phys. **96**, 3939 (1992); Phys. Rev. B **46**, 1853 (1992).
[10] V. Krishna and J. C. Tully, J. Chem. Phys. **125**, 054706 (2006).
[11] B. Hellsing and M. Persson, Phys. Scr. **29**, 360 (1984).
[12] N. Lorente and M. Persson, Faraday Discuss. **117**, 277 (2000).
[13] N. Lorente and H. Ueba, Eur. Phys. J. D **35**, 341 (2005).
[14] M. Head-Gordon and J. C. Tully, J. Chem. Phys. **103**, 10137 (1995).
[15] J. C. Tully, J. Chem. Phys. **73**, 1975 (1980).
[16] A. C. Luntz and M. Persson, J. Chem. Phys. **123**, 074704 (2005).
[17] C. Springer, M. Head-Gordon, and J. C. Tully, Surf. Sci. **320**, L57 (1994).
[18] A. C. Luntz, M. Persson, S. Wagner, C. Frischkorn, and M. Wolf, J. Chem. Phys. **124**, 244702 (2006).
[19] T. Vazhappilly, T. Klamroth, R. Hernandez, and P. Saalfrank, J. Phys. Chem. C **113**, 7790 (2009).
[20] N. Shenvi, S. Roy, P. Parandekar, and J. Tully, J. Chem. Phys. **125**, 154703 (2006).
[21] N. Shenvi, S. Roy, and C. Tully, J. Chem. Phys. **130**, 174107 (2009).
[22] S. Roy, N. A. Shenvi, and J. C. Tully, J. Chem. Phys. **130**, 174716 (2009).
[23] N. Shenvi, S. Roy, and J. C. Tully, Science **326**, 829 (2009).
[24] S. Li and H. Guo, J. Chem. Phys. **117**, 4499 (2002).
[25] G. Katz, Y. Zeiri, and R. Kosloff, J. Phys. Chem. B **109**, 18876 (2005).
[26] P. Saalfrank and R. Kosloff, J. Chem. Phys. **105**, 2441 (1996).
[27] K. Finger and P. Saalfrank, Chem. Phys. Lett. **268**, 291 (1997); P. Saalfrank, G. Boendgen, K. Finger, and L. Pesce, Chem. Phys. **251**, 51 (2000).
[28] T. Klamroth, D. Kröner, and P. Saalfrank, Phys. Rev. B **72**, 205407 (2005).
[29] G.-J. Kroes, Science **321**, 794 (2008).
[30] L. Pesce and P. Saalfrank, Chem. Phys. **219**, 43 (1997).
[31] L. Pesce and P. Saalfrank, J. Chem. Phys. **108**, 3045 (1998).
[32] G. Lindblad, Commun. Math. Phys. **48**, 119 (1976).
[33] Ch. Scheurer and P. Saalfrank, Chem. Phys. Lett. **245**, 201 (1995).
[34] C. C. Marston and G. G. Balint-Kurti, J. Chem. Phys. **91**, 3571 (1989).
[35] M. Berman and R. Kosloff, Comput. Phys. Commun. **63**, 1 (1991).
[36] W. Kohn and L. J. Sham, Phys. Rev. **140**, A1133 (1965).
[37] G. Kresse and J. Furthmuller, Phys. Rev. B **54**, 11169 (1996).
[38] G. Kresse and D. Joubert, Phys. Rev. B **59**, 1758 (1999).
[39] J. P. Perdew and Y. Wang, Phys. Rev. B **45**, 13244 (1992).
[40] H. J. Monkhorst and J. D. Pack, Phys. Rev. B **13**, 5188 (1976).
[41] D. Torres, S. Gonzalez, K. M. Neyman, and F. Illas, Chem. Phys. Lett. **422**, 412 (2006).
[42] D. W. Marquardt, SIAM J. Appl. Math. **11**, 431 (1963).
[43] R. Marquardt and M. Quack, J. Chem. Phys. **109**, 10628 (1998).
[44] H. B. Michaelson, J. Appl. Phys. **48**, 4729 (1977).
[45] J. R. Trail, D. M. Bird, M. Persson, and S. Holloway, J. Chem. Phys. **119**, 4539 (2003).
[46] M. S. Mizielinski, D. M. Bird, M. Persson, and S. Holloway, J. Chem. Phys. **122**, 084710 (2005).
[47] M. Nest and P. Saalfrank, Chem. Phys. **268**, 65 (2001).